

Orally active 4-amino-5-diarylurea-furo[2,3-*d*]pyrimidine derivatives as anti-angiogenic agent inhibiting VEGFR2 and Tie-2

Yasushi Miyazaki,^{a,*} Jun Tang,^b Yutaka Maeda,^a Masato Nakano,^a Liping Wang,^b Robert T. Nolte,^b Hideyuki Sato,^a Masaki Sugai,^a Yuji Okamoto,^a Anne T. Truesdale,^b Daniel F. Hassler,^b Eldridge N. Nartey,^b Denis R. Patrick,^c Maureen L. Ho^c and Kazunori Ozawa^a

^aGlaxoSmithKline, Tsukuba Research Laboratories, 43, Wadai, Tsukuba 300-4247, Ibaraki, Japan

^bGlaxoSmithKline, Five Moore Drive, Research Triangle Park, NC 27709, USA

^cGlaxoSmithKline, Upper Providence R&D, 1250 S. Collegeville Road, Collegeville, PA 19426, USA

Received 3 October 2006; revised 14 December 2006; accepted 14 December 2006

Available online 24 December 2006

Abstract—During our effort to develop dual VEGFR2 and Tie-2 inhibitors as anti-angiogenic agents for cancer therapy, we discovered 4-amino-5-(4-((2-fluoro-5-(trifluoromethyl)phenyl)-aminocarbonylamino)phenyl)furo[2,3-*d*]pyrimidine (**8a**) possessing strong inhibitory activity at both the enzyme and cellular level against VEGFR2 and Tie-2. Compound **8a** demonstrated high pharmacokinetic exposure through oral administration, and showed marked tumor growth inhibition and anti-angiogenic activity in mouse HT-29 xenograft model via once-daily oral administration.

© 2006 Elsevier Ltd. All rights reserved.

Angiogenesis, the formation of new blood vessels from existing vasculature, has been considered a critical event for the growth and metastasis of solid tumors since Folkman first proposed the hypothesis that tumors cannot grow beyond 2–3 mm in the absence of new vasculature.¹ Numerous studies have shown that angiogenic growth factors and cellular kinase receptors regulate a variety of cellular events relating to angiogenic processes. Two growth factor families, VEGFs and Angiopoetins, are of particular interest since their receptors are expressed primarily on endothelial cells and play a direct role in such angiogenic processes.² The VEGFs are required for vasculogenesis and angiogenic sprouting, and act through receptor tyrosine kinases (VEGFR-1, -2, and -3). VEGFR2 mediates endothelial cell proliferation, differentiation, and microvascular permeability.³ The Angiopoetins (Ang-1 and Ang-2), on the other hand, have been implicated in the further remodeling of initial microvasculature and exert biological actions through the Tie-2 receptor.⁴

It is now well established that inhibition of VEGFR2 leads to suppression of angiogenesis and tumor growth. Interference of VEGFR2 signaling with a truncated VEGFR2 gene lacking the kinase domain or inhibition by small molecule inhibitors was shown to significantly suppress the growth of a variety of solid tumors.^{5,6} Similarly, suppression of Tie-2 pathways was also shown to have anti-angiogenic and anti-tumor activities. Antisense reagents of Ang-1 RNA could effectively reduce Ang-1 production and inhibit angiogenesis and tumor growth.⁷ Furthermore, it was shown that interfering with either the VEGFR2 or the Tie-2 pathways led to inhibition of human melanoma xenograft growth.⁸

Based on this body of evidence, we focused on developing small molecules with dual inhibitory activity against both VEGFR2 and Tie-2, expecting the simultaneous inhibition of both enzymes would show synergistic effects through affecting critical stages of blood vessel formation, and thus leading potentially to a new approach to cancer therapy.

From our initial high throughput screen, 4-amino-5,6-bis[(4-methoxyphenyl)furo[2,3-*d*]pyrimidine **1** as identified as a dual inhibitor with moderate potency against both the VEGFR2 and Tie-2 enzymes. Subsequent

Keywords: Kinase inhibitor; Angiogenesis; VEGFR2; Tie-2; Receptor tyrosine kinase.

* Corresponding author. E-mail: yasushi.miyazaki@gsk.com

modification successfully led to 4-amino-5-diarylurea-6-aryl-furo[2,3-*d*]pyrimidines such as compound **2** that exhibits high potency in both VEGFR2 and Tie-2 enzyme and cellular assays (Fig. 1).⁹ In this paper, we describe our further efforts to develop a candidate quality molecule within the 4-amino-5-diarylurea-furo[2,3-*d*]pyrimidine series, possessing both VEGFR2/Tie-2 enzyme and cell dual inhibitory activity, as well as multiple kinase inhibitory profiles affecting angiogenesis. In addition, we report the oral pharmacokinetic exposure and in vivo efficacy of a representative analogue **8a**.

The VEGFR2 X-ray crystal structure of the potent VEGFR2 and Tie-2 dual inhibitor 4-amino-furo[2,3-*d*]pyrimidine **2** showed that among the key interactions the diaryl urea moiety serves as a hook extended into the hydrophobic back pocket of the kinase domain and the aminopyrimidine as an anchor bound to the hinge region. This serves as a basis for the rationale behind the potency observed. Superimposing **2** onto the equally potent dual VEGFR2/Tie-2 inhibitor 5-diarylurea-oxy-benzimidazole derivative **3** on the basis of similar binding motif in the X-ray crystal structure suggested that deleting the 4-methoxyphenyl group at the 6-position of **2** might not affect its potency (Fig. 2).¹⁰ Since such a deletion lowers the molecular weight, this may potentially lead to compounds that show better PK exposure. Moreover, other functional groups can be introduced into the 6-position to fine-tune physicochemical properties such as solubility and lipophilicity, if the need arises. To validate this hypothesis, the 6-position-depleted 4-amino-5-diarylurea-furo[2,3-*d*]pyrimidines were synthesized.

The synthesis is depicted in Scheme 1. 4-Amino-acetophenone **4** was converted to 2-hydroxyacetophenone **5** by bromination and hydroxylation with potassium formate. Subsequent reaction with malononitrile in the presence of diethylamine led to furan **6**, which was treated with triethyl orthoformate, followed by amination and cyclization with sodium ethoxide, providing 4-amino-5-(4-

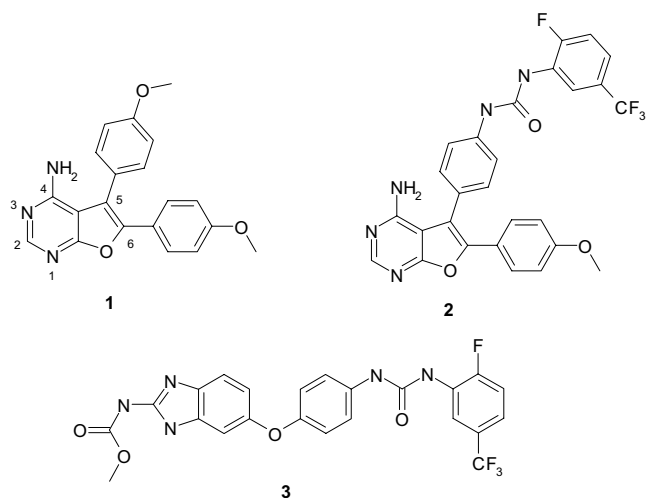


Figure 1. Structure of 4-amino-5,6-diaryl-furo[2,3-*d*]pyrimidine **1**, **2**, and 5-diarylurea-oxy-benzimidazole **3**.

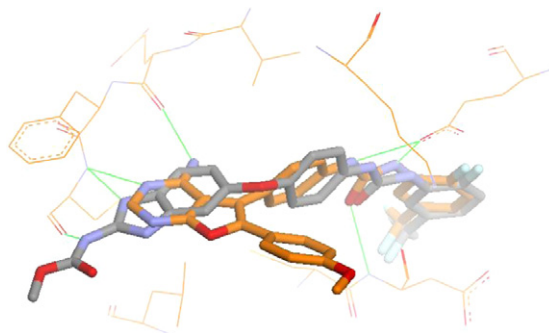
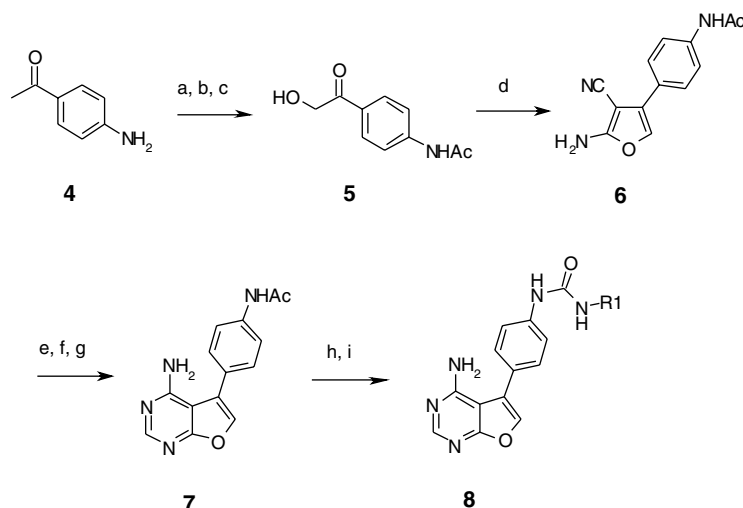


Figure 2. Overlay of 5-diarylurea-oxy-benzimidazole into 4-amino-5-diarylurea-6-aryl-furo[2,3-*d*]pyrimidine complexed with VEGFR2. 5-diarylurea-oxy-benzimidazole **3** (gray) was superimposed into X-ray structure of 4-amino-5-diarylurea-6-aryl-furo[2,3-*d*]pyrimidine **2** complexed (orange) with VEGFR2. Key interactions between inhibitor and protein are shown by green lines.

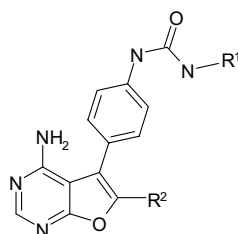
acetamidophenyl)-furo[2,3-*d*]pyrimidine **7**. After removal of the acetyl group, **7** was treated with various isocyanates to provide the corresponding urea derivatives **8**.¹¹

pIC₅₀ values for VEGFR2 and Tie-2 inhibitory activity were determined by HTRF (homogeneous time-resolved fluorescence) method.¹² The catalytic activity of kinases was measured by phosphorylated biotin-peptide conjugate by means of streptavidin linked-APC and europium-labeled anti-phosphotyrosine antibody. As shown in Table 1, deletion of the aryl ring at the 6-position completely retains the enzyme activity comparable to that of the 6-methoxyphenyl analogue **2**. In the preliminary SAR studies of the 4-amino-5,6-diaryl-furo[2,3-*d*]pyrimidine series, both aromatic substituents at 5- and 6-position were deemed important for inhibitory activity;⁹ however, the diarylurea moiety now picks up potency either with or without aromatic substituents at 6-position as suggested from the studies derived from the superimposition with 5-diarylurea-oxy-benzimidazole series. This result suggested that the paramount interactions in the current series are those of the diarylurea with the hydrophobic back pocket and the proton donor/acceptor interactions in the hinge region between the enzymes and the inhibitors.¹³ In Table 1, the SAR of the terminal substitution of the urea portion (R¹) for inhibitory activity against VEGFR2 and Tie-2 is summarized. As shown in the table, 3-trifluoromethylphenyl is important for potency against both VEGFR2 and Tie-2 (compound **8d**). The 17- and 42-fold reduction in potency against Tie-2 and VEGFR2, respectively, of the methoxy analogue **8f** compared to that of **8a** clearly indicated the importance of the hydrophobic interaction between the inhibitor and the hydrophobic amino acid residues of the back pocket. Bulky substituents such as 3-phenoxyphenyl (**8c**) reduced activity against both enzymes, especially for VEGFR2. Introduction of a chloro substituent instead of the fluoro group of **8a** decreases activity against both Tie-2 and VEGFR2 by 16- and 23-fold, respectively (**8e**). Similar reduction in activity was observed by the bulky naphthyl analogues **8g** and 3,5-ditrifluoromethylphenyl **8b**. 2-Naphthyl analogue **8h** increased the potency slightly compared with **8g**,



Scheme 1. Reagents and conditions: (a) Ac_2O , toluene, rt, 96%; (b) Br_2 , AcOH , 60 °C, 63%; (c) potassium formate, NaHCO_3 , $\text{EtOH-H}_2\text{O}$, 40 °C, 50%; (d) malononitrile, Et_2NH , DMF, rt, 81%; (e) HC(OEt)_3 , Ac_2O , 100 °C; (f) NH_3 , EtOH-THF , rt; (g) NaOEt , EtOH-THF , rt, 54% for three steps; (h) 2 M KOH , $\text{EtOH-H}_2\text{O}$, 60 °C, 75%; (i) isocyanates, THF, rt, 95% for 2-fluoro-5-(trifluoromethyl)phenyl isocyanate.

Table 1. VEGFR2 and Tie-2 kinase enzyme inhibition of 4-amino-5-diarylcurea-furo[2,3-*d*]pyrimidines^a



Compound	R ¹	R ²	Tie-2 pIC ₅₀	Tie-2 SD	VEGFR2 pIC ₅₀	VEGFR2 SD
2	2-F-5-CF ₃ -Ph	4-OMe-Ph	ND (8.61) ^b	ND	7.81 (8.56) ^b	<i>n</i> = 1
8a	2-F-5-CF ₃ -Ph	H	7.87 (8.62) ^b	0.29, <i>n</i> = 4	8.11 (8.54) ^b	0.25, <i>n</i> = 6
8b	3,5-Di- CF ₃ -Ph	H	6.42	<i>n</i> = 1	6.86	<i>n</i> = 1
8c	3-Phenoxy-Ph	H	6.39	<i>n</i> = 1	5.76	<i>n</i> = 1
8d	3- CF ₃ -Ph	H	7.99	<i>n</i> = 1	8.15	<i>n</i> = 1
8e	2-Cl-5- CF ₃ -Ph	H	6.69	0.11, <i>n</i> = 3	6.73	0.15, <i>n</i> = 5
8f	2-F-5-OMe-Ph	H	6.65	<i>n</i> = 1	6.48	0.59, <i>n</i> = 2
8g	1-Naphthyl	H	6.74	<i>n</i> = 1	6.35	<i>n</i> = 1
8h	2-Naphthyl	H	7.09	<i>n</i> = 1	7.62	<i>n</i> = 1

^a Number of concentration points per curve for pIC₅₀ determination is 11.

^b The value in the parentheses indicates pIC₅₀ value in a previous assay format.⁹

indicating some space for meta- and para-direction of the terminal phenyl moiety.

Compound **8a** was evaluated for cellular activity based on the growth of human umbilical vein endothelial cells (HUVECs) stimulated by VEGF or the autophosphorylation of c-fms-Tie-2 chimeric receptor transfected into 3T3 cells.⁹ Additionally, cytotoxic assays were conducted using the HFF and HT-29 cell lines.¹⁴ As indicated in Table 2, compound **8a** exhibited potent cellular inhibito-

Table 2. Cellular inhibitory activity of compound **8a** expressed as IC₅₀

Cellular inhibitory activity, IC ₅₀ (nM)			
HUVECV	Tie-2 Autophosphorylation	HFF	HT-29
2.6	18.3	2506	5084

IC₅₀ values are averages from more than two separate experiments.

ry activity against the growth of HUVECs and autophosphorylation of c-fms-Tie-2 chimeric receptor. In addition, there was over 900-fold selectivity between inhibition of growth of HUVECs and HFF cell lines,

Table 3. Systemic exposure via oral administration in the male CD-1 mouse of compound **8a**

Systemic exposure in mice (10.7 mg/kg, po)			
<i>C</i> _{max} (ng/mL)	<i>T</i> _{max} ^a (min)	AUC _{0-t} (min µg/mL)	DNAUC _{0-t} (min kg/L)
2724 ± 588	480, 120, 120, 120	1201 ± 272	112 ± 22

Abbreviations: *C*_{max}, maximum blood concentration attained after oral gavage; *T*_{max}, time *C*_{max} was attained; AUC_{0-t}, area under the blood concentration–time curve truncated to the last time point with measurable concentrations; DNAUC_{0-t}, dose-normalized AUC.

^a Individual values shown due to variability.

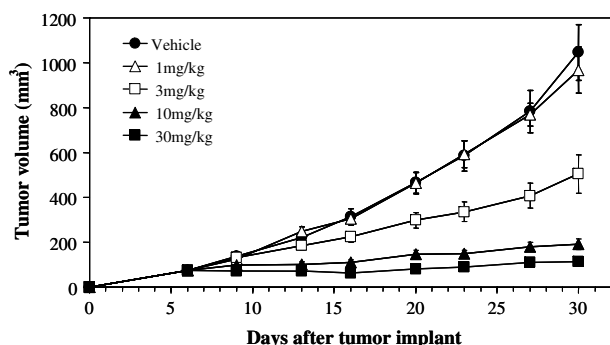


Figure 3. Effect of **8a** or vehicle on HT-29 tumor growth in xenograft model. HT-29 human adenocarcinoma cells (2×10^6 cells) were implanted sc in the flank of female CD-1 nude mice. Five days after the implantation, once-daily oral treatment with **8a** or vehicle (1% CMC-Na/saline) was started and continued for the experimental period. Data points represent a means \pm SE ($n = 8$).

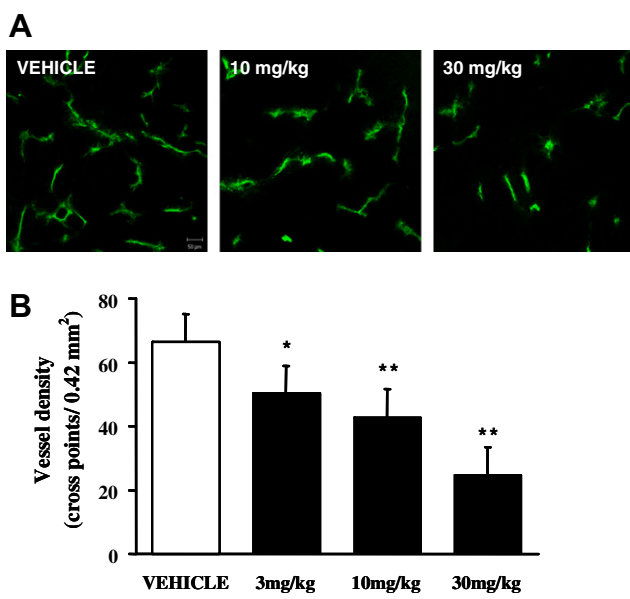


Figure 4. Effect of **8a** on vascular density in HT-29 tumor xenografts. A view of the square field (686- μ m width) on frozen section was scanned with a confocal laser-scanning microscope (A), and the vessel density (B) in 'angiogenic hot spots' was determined by image analysis according to the method described by Rieder et al.¹⁴. The column with bar represents a means \pm SE ($n = 4$). * and ** indicate $p < 0.05$ and $p < 0.01$, respectively, as compared to VEHICLE group (Dunnett's multiple comparison test).

suggesting that general cytotoxicity is not the mechanism for inhibition of HUVEC growth. Preliminary pharmacokinetic studies in mouse at a dose of approximately 10 mg/kg of compound **8a** formulated with

CMC-Na/saline showed excellent exposure after oral administration (Table 3).¹⁵

In vivo anti-tumor activity of compound **8a** was evaluated in a mouse HT-29 tumor xenograft model. HT-29 human colon adenocarcinoma cells were cultured and implanted into nude mice and 5 or 6 days later tumor size and volume were measured. Compound **8a** was suspended in 1% carboxymethylcellulose sodium salt saline solution (1% CMC-Na/saline) and orally administered at doses of 1, 3, 10, and 30 mg/kg once daily. For the control, 1% CMC-Na/saline was given. Through the experimental period, the tumor volume and the body weight were monitored. As shown in Figure 3, oral administration of compound **8a** at 1–30 mg/kg dose-dependently inhibited HT-29 tumor growth. At 30 mg/kg tumor growth was almost completely suppressed, although the body weight loss was observed during the late stage of the experimental period. Nevertheless, at doses of 3 and 10 mg/kg the tumor growth was significantly inhibited without body weight loss.

Anti-angiogenic activity of compound **8a** was also examined in mouse HT-29 tumor xenograft model at doses of 3, 10, and 30 mg/kg or vehicle (1% CMC-Na/saline) for 6 days. Vascular endothelial cells in HT-29 xenografts were labeled with FITC-lectin and blood vessels in the section of 'angiogenic hot spots', which are the most densely vascularized areas of the tumor, were detected as fluorescent images by confocal laser-scanning microscopy. Blood vessel images were digitized and quantified according to the method described by Rieder et al.¹⁶ in which the vascular density was determined by the number of the cross points between digitized vessel images and computer-generated grid (40 μ m-interval). Once-daily oral treatment of HT-29 tumor bearing mice with **8a** decreased blood vessels (Fig. 4A), and anti-angiogenic activity of **8a** was dose-dependent between 3 and 30 mg/kg (Fig. 4B). Vessel density in the tumor section was significantly inhibited 24.3%, 35.6%, and 62.9% by 3, 10, and 30 mg/kg of **8a**, respectively. In addition, the growth of the xenografted tumors was also inhibited during the 6 days of treatment.

Recently, compounds with multiplexed kinase inhibitory profiles have demonstrated efficacy in clinical trials.¹⁷ In fact, recent FDA approval of sorafenib (Nexavar®) which inhibits VEGFR2 plus complementary and additional targets, such as b-Raf and PDGF, would support pursuing a multiplexed kinase inhibitory profile strategy. Compound **8a** was evaluated in a kinase screening panel and demonstrated inhibitory activity against multiple kinases such as VEGFR1, VEGFR3, and PDGFR, which are important kinases required

Table 4. Kinase panel selectivity profile of compound **8a**. Potency is represented by pIC₅₀ value^a

Akt3	CDK2	EGFR	GSK3	SRC	c-FMS	PDGFR	VEGFR1	VEGFR3
4.76 (0.62, $n = 2$)	4.75 (0.31, $n = 7$)	5.0 (0, $n = 2$)	5.66 (0.1, $n = 2$)	6.27 (0.45, $n = 6$)	7.41 (0.32, $n = 2$)	7.56 (0.39, $n = 5$)	8.07 (0.42, $n = 2$)	8.12 (0.20, $n = 2$)

^a Standard deviation and n values are given in parentheses (n , replicates).

for angiogenesis. The profile data of compound **8a** are shown in Table 4.¹⁸

In conclusion, as a part of our research for anti-angiogenic agents for cancer therapy, we synthesized 4-amino-furo[2,3-*d*]pyrimidine derivatives, and evaluated their activities as VEGFR2 and Tie-2 kinase inhibitors. Compound **8a** exhibited not only potency in both enzyme and cellular assays, but also exhibited anti-angiogenic and anti-tumor activity in HT-29 tumor xenograft models. These results indicate that compounds of furopyrimidines bearing diarylurea moieties potentially possess promising features as drug candidates for anti-angiogenic cancer therapy.

Acknowledgments

We acknowledge Michael Hansbury and Roberta Batorisky for their assistance with the Tie-2 autophosphorylation results and Ron Wegrzyn, Hieu Do, Kevin Kershner, and Jessica Ward for their contribution to the HFF and HT-29 proliferation data. We acknowledge CVU Preclinical Drug Discovery DMPK for measurement of systemic exposure, Screening & Compound Profiling for kinase panel assays. The authors thank Joseph H. Chan, Karen E. Lackey, and Stephen V. Frye for their guidance and support.

Supplementary data

Supplementary data associated with this article can be found, in the online version, at doi:10.1016/j.bmcl.2006.12.077.

References and notes

- Folkman, J. N. *Engl. J. Med.* **1971**, *285*, 1182.
- Yancopoulos, G. D.; Davis, S.; Gale, N. W.; Rudge, J. S.; Wiegand, S. J.; Holash, J. *Nature* **2000**, *407*, 242.
- Veikkola, T.; Karkkainen, M.; Claesson-Welsh, L.; Alitalo, K. *Cancer Res.* **2000**, *60*, 203.
- Jones, N.; Iljin, K.; Dumont, D. J.; Alitalo, K. *Nat. Rev. Mol. Cell Biol.* **2001**, *2*, 257.
- Millauer, B.; Longhi, M. P.; Plate, K. H.; Shawver, L. K.; Risau, W.; Ullrich, A.; Strawn, L. M. *Cancer Res.* **1996**, *56*, 1615.
- Wedge, S. R.; Ogilvie, D. J.; Dukes, M.; Kendrew, J.; Curwen, J. O.; Hennequin, L. F.; Thomas, A. P.; Stokes, E. S.; Curry, B.; Richmond, G. H.; Wadsworth, P. F. *Cancer Res.* **2000**, *60*, 970.
- Shim, W. S.; Teh, M.; Mack, P. O.; Ge, R. *Int. J. Cancer* **2001**, *94*, 6.
- Siemeister, G.; Schirner, M.; Weindel, K.; Reusch, P.; Menrad, A.; Marme, D.; Martiny-Baron, G. *Cancer Res.* **1999**, *59*, 3185.
- Miyazaki, Y.; Matsunaga, S.; Tang, J.; Maeda, Y.; Nakano, M.; Philippe, R. J.; Shibahara, M.; Liu, W.; Sato, H.; Wang, L.; Nolte, R. T. *Bioorg. Med. Chem. Lett.* **2005**, *15*, 2203.
- Cheung, M.; Harris, P. A.; Hasegawa, M.; Ida S.; Kano K.; Nishigaki N.; Sato, H.; Veal, J. M.; Washio, Y.; West, R. I. PCT Application, WO2002044156.
- Analytical data of compound **8a**: ¹H NMR (400 MHz, DMSO-*d*₆) ppm 7.39–7.42 (m, 1H), 7.47 (d, *J* = 8.6 Hz, 2H), 7.49–7.54 (m, 1H), 7.63 (d, *J* = 8.8 Hz, 2H), 7.95 (s, 1H), 8.26 (s, 1H), 8.63 (d, *J* = 7.1 Hz, 1H), 8.99 (s, 1H), 9.39 (s, 1H). LC/MS: *m/z* 432 (M + 1)⁺, 430 (M – 1)[–].
- HTRF is based on the proximity of a donor label (europium chelate) and acceptor label (allophycocyanin, APC) which have been brought together by a specific binding reaction. When the two entities come into close proximity and upon excitation, energy transfer occurs and APC emits a specific long-lived fluorescence at 665 nm. The kinases were purified as the intracellular domain of human Tie-2 or VEGFR2 fused by GST and/or 6× His tags. In the case of VEGFR2, the enzyme contains both GST and 6×His tags. The catalytic activity of each kinase was detected by using a biotinylated synthetic peptide as a substrate, biotin-C6-LEARLVAYEGWVAGKKK-amide, and biotin-aminohexyl-EEEEYFELVAKKKK-NH₂, for Tie-2 and VEGFR2, respectively. Phosphorylated substrate is measured by streptavidin linked-APC (Molecular Probes) and europium-labeled anti-phosphorylated tyrosine antibody (Perkin-Elmer). Assay conditions are as follows. Tie-2: GST-Tie-2 was preactivated with 800 μM ATP, 1 mM DTT, 0.1 mg/mL BSA, 10 mM MgCl₂, 0.01% Tween 20 in 100 mM HEPES, pH 7.5, for 1–2 h. The preactivated enzyme was then incubated for 1–3 h with 1 μM peptide, 20 μM ATP, 5 mM MgCl₂, 1 mM DTT, 0.1 mg/mL BSA, 0.01% Tween 20, and test compound in 100 mM HEPES, pH 7.4. VEGFR2: GST-6× His-VEGFR2 was preactivated with 100 μM ATP, 0.3 mM DTT, 0.1 mg/mL BSA, and 10 mM MgCl₂ in 100 mM HEPES, pH 7.5, for 20 min. The preactivated enzyme was then incubated for 90 min. with 360 nM peptide, 50 μM ATP, 10 mM MgCl₂, 0.3 mM DTT, 0.1 mg/ml BSA and test compound in 100 mM HEPES, pH 7.5.
- Dai, Y.; Guo, Y.; Frey, R. R.; Ji, Z.; Curtin, M. L.; Ahmed, A. A.; Albert, D. H.; Arnold, L.; Arries, S. S.; Barlozzari, T.; Bauch, J. L.; Bouska, J. J.; Bousquet, P. F.; Cunha, G. A.; Glaser, K. B.; Guo, J.; Li, J.; Marcotte, P. A.; Marsh, K. C.; Moskey, M. D.; Pease, L. J.; Stewart, K. D.; Stoll, V. S.; Tapang, P.; Wishart, N.; Davidsen, S. K.; Michaelides, M. R. *J. Med. Chem.* **2005**, *48*, 6066.
- HFF or HT-29 cells (ATCC) were cultured in DMEM, 10% FBS, high glucose, and L-glutamine. Logarithmically growing cells were seeded into 96-well plates (Nunclon polystyrene white part No. 136102) at 500 cells per well and allowed to adhere overnight at 37 °C in a humidified 5% CO₂ incubator. Compounds were dissolved in 100% DMSO and serially diluted twofold for 20 points. Compounds were diluted into DMEM, then diluted into the cell plates at a final dilution of 1:500 yielding a final DMSO concentration of 0.2%. Plates were incubated for three days and then developed with Promega CellTiter-Glo reagent and read on a Perkin-Elmer Victor V plate reader. Curves are fit to a four parameter model using XLfit and the inflection point is recorded as the EC₅₀.
- In another preliminary PK experiment, compound **8a** showed better exposure compared with compound **2** on C_{max} and AUC (limited) by 1.9- and 2.6-fold, respectively.
- Rieder, M. J.; O'Drobinak, D. M.; Greene, A. S. *Microvasc. Res.* **1995**, *49*, 180.
- Adams, J.; Huang, P.; Patrick, D. *Curr. Opin. Chem. Biol.* **2002**, *6*, 486.

18. Davis, S. P.; Reddy, H.; Caivono, M.; Cohen, P. *Biochem. J.* **2000**, 351, 95, Compound **2** generally showed similar selectivity profile with compound **8a** (IC_{50} are $>10\ \mu M$ against CDK2, EGFR, GSK3 and $<100\ nM$ against SRC and VEGFR3) as far as the inhibitory activity was measured. However, it was found that some substituents on 6-position could change selectivity profile on certain targets (data are not shown).